Available online at www.sciencedirect.com
ScienceDirect
Journal of Molecular Graphics and Modelling 26 (2008) 991–1003
Journal of Molecular Graphics and Modelling
www.elsevier.com/locate/JMGM

Modeling binding modes of angiotensin II and pseudopeptide analogues to the AT_2 receptor

Christian Sköld [a], Gregory Nikiforovich [b], Anders Karlén [a,*]

[a] *Department of Medicinal Chemistry, Division of Organic Pharmaceutical Chemistry, BMC, Uppsala University, P.O. Box 574, SE-751 23 Uppsala, Sweden*
[b] *Department of Biochemistry and Molecular Biophysics, Washington University School of Medicine, 700 S. Euclid Avenue, St. Louis, MO 63110, USA*

Received 28 May 2007; received in revised form 16 August 2007; accepted 21 August 2007
Available online 26 August 2007

Abstract

The 3D model of the AT_2 receptor has been built employing homology to the transmembrane domain of rhodopsin and a novel build-up procedure for restoring the extracellular loops. By docking a model peptide of angiotensin II in the AT_2 receptor model two plausible binding modes were identified. These binding modes were in agreement with most of the suggested ligand–receptor contact points reported in the literature. Eight active and one inactive pseudopeptide angiotensin II analogue were also docked in the receptor and four of the active pseudopeptides were found to mimic the binding mode of angiotensin II. An alternative binding mode for the other four active pseudopeptides was found.

Keywords: AT_2 receptor; Angiotensin II; Homology modeling; Docking; Bioactive conformation

1. Introduction

The octapeptide angiotensin II (Ang II, Asp-Arg-Val-Tyr-Ile-His-Pro-Phe) acts on two receptors in the renin–angiotensin system (RAS), the AT_1 and the AT_2 receptors. The AT_1 receptor mediates the well-known effects of Ang II, such as regulation of blood pressure and electrolyte and water retention. The physiological role of the AT_2 receptor is still under investigation and has been linked to processes such as apoptosis, tissue repair, and fetal development [1,2]. Both of the receptors belong to the same class of the seven transmembrane domain G protein-coupled receptors (GPCRs) but share only 32–34% sequence identity [3,4].

The conformation of Ang II when bound to the AT_1 receptor has been thoroughly investigated earlier with most results indicating that Ang II adopts a turn conformation around the Tyr residue [5–14]. Photoaffinity labeling studies combined with homology modeling have suggested, however, that Ang II binds to the AT_1 receptor in an extended conformation [15,16].

The binding conformation of Ang II when interacting with the AT_2 receptor has been investigated to a lesser extent, but mono- and bi-cyclizations, including turn mimicking structures, in the 3–5 region of Ang II have produced analogues with retained affinity [7,17–21]. An extended receptor-bound conformation of Ang II has also been suggested in the case of AT_2 binding [16]. Two independent amino acid scans of Ang II have shown that modification of most of the side chains do not drastically affect the affinity to the AT_2 receptor [22,23]. The side chains most sensitive to modification in both studies were the Arg and His side chains, followed by Tyr. In one of the studies amidation of the Phe carboxyl group was performed, which also resulted in a peptide with decreased affinity to the AT_2 receptor [23].

Point-mutation studies of the AT_2 receptor performed by several groups have found amino acid residues in the receptor important for affinity of different ligands. Arg^{182} [24,25], Lys^{215} [26,27], His^{273} [28], Asp^{297} [25,29], and Asp^{279} [30], have been shown to affect affinity of Ang II and Ang II analogues to the AT_2 receptor (for easier notation we herein refer to non-numbered amino acids as part of ligands and numbered amino acids as part of the AT_2 receptor). Notably, the site-directed mutagenesis studies performed for the

* Corresponding author. Tel.: +46 18 471 4293; fax: +46 18 471 4474.
E-mail address: anders.karlen@orgfarm.uu.se (A. Karlén).

1093-3263/$ – see front matter
doi:10.1016/j.jmgm.2007.08.005

AT_2 receptor were mainly limited to positions occupied by important residues in the homologous AT_1 receptor. Also, these conserved receptor residues are suggested to interact with the same Ang II residues in both AT_1 and AT_2 receptor binding. In more direct experiments, Escher and co-workers have used photoaffinity labeling to identify contact points between Ang II analogues and the AT_2 receptor. Their results suggested that Val is in the vicinity of the N-terminal segment, in proximity of Ile^{14}, of the AT_2 receptor and that Phe is within 6–7 Å of the Met^{128} and Met^{138} in the receptor and that Ang II is binding in an extended conformation to reach these contact points [16,31,32]. Fig. 1 presents a schematic overview of the investigated AT_2 receptor residues and suggested Ang II–AT_2 receptor contact points.

We have previously derived models of the binding mode of several constrained pseudopeptide Ang II analogues to the AT_2 receptor using a ligand-based approach [18–21]. In the present study we aim to explore the ligand binding mode of both the pseudopeptides and the native ligand in the environment of the receptor. Since experimental 3D structures of neither the AT_1 nor the AT_2 receptor are currently available, modeling is the only way to build the plausible 3D models of the AT_2 receptor. Both the AT_1 and AT_2 receptor belong to the same GPCR family as the photoreceptor rhodopsin (family A) [33]. The high resolution X-ray structure of the bovine rhodopsin receptor, first published by Palczewski et al. [34], has been used as a template for several homology modeling studies of GCPRs, including the AT_1 and AT_2 receptors [16,35,36]. However, there is no pronounced sequence homology between the extracellular region of rhodopsin and those of the AT_1 and AT_2 receptors, which means that the conformational preferences for the extracellular loops of the AT_1 and AT_2 receptors may be quite different from the snapshot provided by the X-ray structure of rhodopsin. Therefore, a more detailed study of the binding of Ang II and Ang II analogues should also account for the conformational flexibility of the extracellular domain of the receptor as well as for the flexibility of the ligands. Accordingly, the aims of this study were first, to build a homology model of the transmembrane (TM) region of the AT_2 receptor using the bovine rhodopsin as a template structure; second, to explore the conformations of the extracellular loops to find suitable conformations allowing docking of Ang II; third, to explore the binding mode of Ang II in the receptor; fourth, to explore the binding mode of pseudopeptide ligands in the receptor.

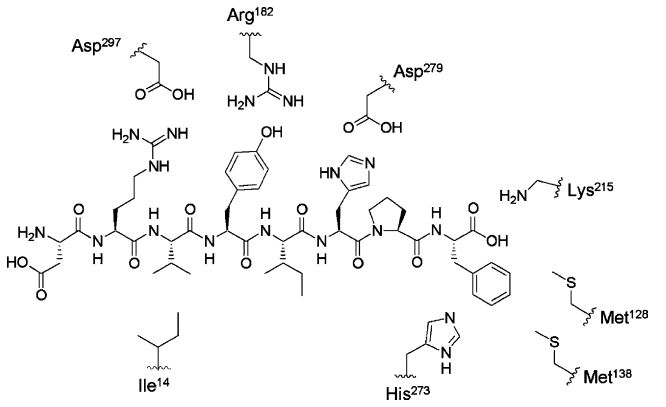

Fig. 1. Ang II and reported AT_2 receptor residues possibly involved in binding. The positioning of the residues reflects the suggested ligand–receptor contacts as well as residues that are close to the Ang II binding pocket. For Arg^{182}, Lys^{215}, His^{273}, and Asp^{279} the suggested contacts are from Ang II interactions with conserved amino acids in the AT_1 receptor.

2. Experimental methods

2.1. Building the AT_2 receptor model

Molecular modeling procedures for building the 3D model of the transmembrane (TM) region of the AT_2 receptor and restoring the extracellular loops (ECL) were the same as were applied earlier for building the 3D model of rhodopsin [37,38]. All energy calculations were performed with the ECEPP/2 force field [39,40], employing rigid valence geometry and using a dielectric constant of 80.0 to reduce possible excessive interactions between the charged groups. Only the *trans*-conformation of the amide bonds was considered, and Arg, Lys, Glu, and Asp residues were modeled as charged species. The His residues were built with the hydrogen atom bonded to the N_π atom. The N- and C-termini of each helix were capped with acetyl- and NHMe-groups, respectively.

The strategy used in this study for building and validating the AT_2 receptor model consisted of the following steps: (1) build the seven TM helical fragments of the AT_2 receptor starting from rhodopsin, and (2) build the extracellular loops (ECL1–ECL3) in energetically favorable positions. The intracellular loops of the AT_2 receptor were not considered, since they would not influence binding of ligands accessing the extracellular loops. Furthermore the N-terminal tail of the receptor was not considered because of its high flexibility. Therefore, the AT_2 receptor model built in this study should be regarded as a partial AT_2 receptor model.

2.1.1. Transmembrane region

The 3D structure of the TM region of the rat AT_2 receptor was built based on the X-ray structure of bovine rhodopsin [34] (PDB entry 1F88). First, the TM helical fragments of the AT_2 receptor were defined by sequence homology to the rhodopsin helices found by the ClustalW procedure [41] as follows: TM1, E45–I57–C70 (the first, middle and last residue, respectively); TM2, S79–L92–Y106; TM3, V115–A130–V146; TM4, N156–V167–F179; TM5, S208–F220–G233; TM6, T250–F265–L281; and TM7, A299–F308–Y318. The sequence alignment can be found in the supporting information. Then, the helical fragments of the AT_2 receptor were assembled in a TM helical bundle based on the following procedure: (i) determining the conformation of each individual helix by optimization of the side chain torsions and energy minimization involving all dihedral angles, (ii) superimposing the obtained helix conformations over the X-ray structure of rhodopsin (C_α atoms only) according to the alignment, and (iii) packing the seven helices into the energetically best arrangement while keeping the dihedral angles of the helical backbone fixed in the

values obtained for the individual helices (step (i)). These steps are further described below.

(i) Energy minimization for each individual TM helix of the AT_2 receptor started from the backbone conformation (ϕ, ψ, and ω dihedral angles) of the corresponding rhodopsin helix (PDB entry 1F88A). The ϕ and ψ angles were allowed to rotate with the limitation $-60 \pm 40^\circ$ that to some extent mimics the maximal limitations on intrahelical mobility of TM helices immobilized in the membrane; most dihedral angle values found in the X-ray structures of TM helical fragments do not exceed these limitations [34]. For the same reason, the ω angle in Pro residues was limited to a value of $180 \pm 30^\circ$. Side chain torsions were optimized before and after energy minimization by an algorithm developed earlier [42]. Due to an obvious distortion in the helical structure of TM6 after this minimization procedure, the starting ϕ, ψ-values for Tyr^{269} were changed to -100°, -60° to keep its backbone angles within the limits.

(ii) For each individual helix, the obtained structures differed from the corresponding helices in rhodopsin by the rms values 1.2 Å (TM1), 2.1 Å (TM2), 1.3 Å (TM3), 1.6 Å (TM4), 1.9 Å (TM5), 0.9 Å (TM6), and 1.7 Å (TM7); all rms values were calculated for positions of C_α atoms only.

(iii) Packing of the seven TM helices into the bundle consisted of minimization of the sum of all intra- and inter-helical interatomic energies in their multi-dimensional parameter space. These included the $6 \times 7 = 42$ ''global'' parameters (related to movement of the individual helices as rigid bodies, namely, translations along the coordinate axes *X*, *Y*, *Z*, and rotations around these axes, T_x, T_y, and T_z) and the ''local'' parameters (the dihedral angles of the amino acid side chains in all helices). Side chain torsions were optimized prior to each energy minimization step by an algorithm described earlier [42]. Energy minimization proceeded until reaching the convergence criterion of $\Delta E < 1$ kcal/mol. The coordinate system for the global parameters was selected as follows: the long axial *X* coordinate axis for each TM helix was directed from the first to the last C_α atom; the *Y*-axis was perpendicular to *X* and traversed through the C_α atom of the ''middle'' residue of each helix; and the *Z*-axis was built perpendicular to *X* and *Y* to maintain the right-handed coordinate system. The resulting 3D structure differed from the TM bundle of rhodopsin by 1.9 Å (rms distance of the C_α atoms).

2.1.2. Extracellular loops

The obtained structure of the TM region of the AT_2 receptor was used as a template for restoring possible 3D structures of the external loops connecting TM2 and TM3 (ECL1, fragment 106–115), TM4 and TM5 (ECL2, 179–208) and TM6 and TM7 (ECL3, 281–299). The N-terminal fragment of the receptor was not included in the modeling procedure. All loops were mounted on the template by adding three residues before and after the loop fragment and overlapping C_α atoms for the first and last four residues of the loop fragment with the corresponding C_α atoms in the stems of the TM helices. First, geometrical sampling of the individual loops was performed starting from the smallest loop to the largest, i.e., from ECL1 to ECL3 to ECL2. As soon as the resulting structures of the smaller loop were selected, the loop structure closest to the average spatial positions of the C_α atoms was included in the template, providing additional geometrical limitations for thelarger loops. The sampling was basically a stepwise elongation of the loop covering all combinations of the possible backbone conformations for the stepwise growing loops. Starting conformations of individual residues and overall sampling procedure were as described earlier [38] with limitations on the residue–residue contacts within the loop (C_α–C_α distances greater than 4 Å) and on the contacts between the loop and the template (C_α–C_α distances greater than either 6 or 8 Å). The values of the EL coefficient ranged from 1.0 to 3.0 and the DEL coefficient was 0.0 (for an explanation of the coefficients see [38]). The specific values of the coefficients were selected to keep the number of structures to consider at each elongation step between 100 and 500,000. Elongation steps were as follows: a single step from residue 106 to residue 115 for ECL1; sequential steps from 281 to 290 to 292 to 294 to 296 to 299 for ECL3; and steps from 179 to 188 to 190 to 192 to 195 to 197 to 199 to 202 to 204 to 208 for ECL2. In the case of ECL2, an additional limitation imposed by the conserved disulfide bridge Cys^{117}-Cys^{195} was employed by limiting C_α–C_α distances from the helical stems of TM4 and TM5 to Cys^{195} to the values of the corresponding distances to Cys^{187} in rhodopsin.

In total, geometrical sampling selected 634 potentially loop-closing backbone conformations for ECL1; 38381 for ECL3; and 592 conformations for ECL2. Then, the selected structures for each individual loop were subjected to energy minimization employing the ECEPP/2 force field; the dielectric constant was set at 80 to mimic to some extent the water environment of the protruding loops. All parameters employed for energy minimization were as described previously [38]. The energy minimizations yielded 35 low-energy structures ($\Delta E \leq 8$ kcal/mol), which were divided into seven clusters of similar structures (defined by an rms distance ≤ 2 Å, C_α-atoms only) for ECL1; 81 structures within $\Delta E \leq 19$ kcal/mol falling into 69 (38) different clusters for ECL3 (the number in parenthesis correspond to clustering with the rms distance of 3 Å); and 52 structures within $\Delta E \leq 40$ kcal/mol falling into 27 (9) different clusters for ECL2. The energy cut-off values were arbitrarily chosen, but roughly followed 1 kcal/mol per residue [43]. The elevated energy cut-off for ECL2 was used to compensate for the unexpectedly high-energy gap between the lowest energy structure and the second lowest energy one, which otherwise might cause a drastic decrease of the number of selected low-energy conformations.

The lowest-energy conformers in each cluster were selected as representatives for further consideration in the extracellular ''package'' comprising all combinations of conformations for ECL1 + ECL2 + ECL3 ($7 \times 9 \times 38 = 2394$ combinations). Then, for all combinations, energy minimizations were performed with the same limitations as those described earlier [38]. Three hundred and seventy-three combinations were finally selected using an energy cut-off of 50 kcal/mol, which were divided into nine structural clusters, based on the

"global" rms distance cut-off of 2 Å (the heavy atoms of the backbone) overlapping only the residues corresponding to the helical stems. The AT_2 receptor model that had the most open conformation with respect to the extracellular loops was selected for further studies.

2.2. Refinement of the AT_2 receptor model

This step consisted of (1) identification of a possible receptor-bound conformation of Ang II, (2) constrained docking of Ang II in the receptor starting from this conformation, and (3) refinement of the positioning of the extracellular loops by also including the docked ligand in the build-up procedure of the loops.

2.2.1. Receptor-bound conformation of Ang II

Before refining the extracellular loops a plausible starting conformation of Ang II that reflected the receptor-bound conformation was needed since this conformation indirectly guides the positioning of the loops. To generate this starting conformation we first performed independent energy calculations using a previously described build-up procedure [14] on four peptides with high AT_2 receptor affinity, namely Ang II (K_i = 0.6 nM), Asp-Arg-*cyclo*(Pen-Tyr-Pen)-His-Pro-Phe (K_i = 6.2 nM), Asp-Arg-*cyclo*(Cys[CH_2]-Tyr-Cys)-His-Pro-Phe (K_i = 0.6 nM), and Asp-Arg-*cyclo*(Cys[CH_2]-Tyr-homoCys)-His-Pro-Phe (K_i = 1.6 nM) [44]. For Ang II, the Ile residue was replaced by Val in the modeling. For each peptide, the build-up procedure and energy minimization generated the set of low-energy backbone conformations within 8 kcal/mol of the lowest energy conformation, with the spatial positions of the side chains optimized according to a previously developed algorithm [42]. Geometrical comparison of the sets showed that they included two families of low-energy conformers similar for all four peptides at the rms level <1.5 Å when Asp was excluded (C_α atoms for residues 2–8). One of the conformational families was more extended, and the other more folded. The conformation of Ang II in either of these families could be a candidate for binding to the AT_2 receptor. Interestingly, both families were very different from the suggested AT_1 receptor binding conformation of Ang II, which has been deduced by molecular modeling earlier [14]. Since some experimental data support the extended conformation of Ang II in complex with the AT_2 receptor [16] and because of the significant distance between the AT_2 receptor residues Asp^{297} and Lys^{215} in our model, which are suggested contact points for Ang II [25–27,29], the extended conformer was selected for further docking to the 3D model of the receptor. The dihedral angles of the backbone atoms defining this conformer (residues 2–8) are listed in Table 1 (conformation 1).

2.2.2. Initial docking of Ang II to the AT_2 receptor

The derived AT_2 receptor structure was first minimized within MacroModel [45] with the amino acid backbone of the receptor frozen. The OPLS-AA/L force field [46] as implemented in MacroModel (OPLS 2005) was used with a dielectric constant of 1. For energy minimization, truncated newton conjugate gradient (TNCG) [47] with a maximum of 500 steps and a convergence criterion of 0.5 kJ mol^{-1} $Å^{-1}$ was used. After this initial minimization ECL2 had to be removed from the AT_2 receptor model to create an opening for the ligand and to form a tentative binding pocket based on the suggested Ang II–AT_2 receptor contact points.

Since no consensus of the orientation of the Asp residue was found between the peptides in the generation of the possible binding conformation described above (conformation 1 in Table 1), this residue was removed to form a model peptide of Ang II (Arg-Val-Tyr-Val-His-Pro-Phe), used as ligand in the docking study. The Arg guanidino group and the Phe carboxyl group were built as charged species but to reduce any strong electrostatic interactions specific for the model peptide the N-terminal amine was left uncharged. The ligand was manually docked in the tentative binding pocket in the receptor guided by the suggested Arg-Asp^{297} and Phe-Lys^{215} contacts and with a minimum of steric clashes. Two distance constraints (4 ± 1 Å with a force constant of 100 kJ mol^{-1} $Å^{-2}$), representing the possible $C_{guanidino,Arg}$–$C_{carboxyl,Asp297}$ and $C_{carboxyl,Phe}$–$N_{amine,Lys215}$ ionic bridges, were introduced to preserve these contact points in the docking. The docking was performed using the Monte Carlo multiple-minimum (MCMM) [48,49] search protocol in MacroModel. The ligand and the side chain atoms of Lys^{215}, His^{273}, Asp^{279}, Asp^{297}, and Lys^{118} were allowed to move in the analysis (Lys^{118} was included because the position of this side chain was severely affected by the now removed ECL2). The side chain atoms of residues within 10 Å of the moving atoms were fixed with a force constant of 200 kJ/mol, but their mutual interactions were kept in the energy calculations (debug switch 17 in BatchMin). The backbone atoms within 10 Å of the moving atoms were frozen during the calculation. The torsion angles and ligand movement were searched with 1000 MCMM steps, altering 1–28 d.o.f. in each step. Energy minimization was performed using TNCG with a maximum of 500 steps and a convergence criterion of 1.0 kJ $Å^{-1}$ mol^{-1}. The OPLS 2005 force field was used with a dielectric constant of 1.0.

Table 1
Backbone dihedral angles (in degrees) of presented conformations of the Ang II model peptide

Conformation	Arg		Val		Tyr		Val (Ile)		His		Pro		Phe	
	ϕ	ψ	ϕ	ψ	ϕ	ψ	ϕ	ψ	ϕ	ψ	ϕ	ψ	ϕ	ψ
1	–	175	−84	108	−110	10	−84	−31	54	74	−75	73	−137	–
2	–	149	−84	140	−84	70	−79	58	−40	99	−98	10	−158	–
3	–	142	−84	141	−86	71	−72	55	−45	108	−96	27	92	–

Conformations within 100 kJ/mol of the energy minimum were saved. The criterion for unique conformations was a minimum atomic separation of 1.5 Å when comparing the position of all heavy atoms of the ligand and the $C_{carboxyl,Asp297}$, $C_{carboxyl,Asp279}$, $N_{amine,Lys215}$, $N_{amine,Lys118}$, and $C_{\gamma,His273}$ atoms of the receptor.

2.2.3. Refinement of the extracellular domain

When the 10 lowest energy docking poses of the ligand (corresponding to $\Delta E = 8$ kcal/mol) were examined it appeared that the previously selected ''most open'' conformation of ECL2 may well tolerate the poses except for some possible steric clash of the ligand with residues 188–199 in the center of the loop. Therefore, this portion of ECL2 was rebuilt starting from the receptor model that included ECL1, ECL3, and ECL2 (fragments 179–188 and 199–208) as well as Ang II according to the previously described procedure. The rebuilding procedure was performed as previously described, with elongation steps from residue 188 to 195 to 199 in ECL2, which yielded 123 backbone structures for further consideration. The subsequent energy minimization found 18 low-energy conformations ($\Delta E \leq 12$ kcal/mol) that satisfied an additional limitation imposed by the disulfide bridge Cys^{117}-Cys^{195}. The conformations were then divided into four clusters by an rms distance cut-off of 2 Å and the one that could best accommodate the poses of the ligand was added to the final 3D model of the AT_2 receptor. To prepare the receptor for further analysis, the ligand was removed from the complex and the spatial positions of the amino acid side chains of the receptor were redefined by energy minimization to convergence (0.5 kJ mol^{-1} $Å^{-1}$) in the OPLS 2005 force field and now also using the generalized-born/surface-area (GB/SA) water solvation model [50] implemented in MacroModel. The amino acid backbone of the receptor was frozen during the minimization.

2.3. Ligand docking to the final AT_2 receptor model

The next step in this study consisted of (1) unconstrained docking of the Ang II model peptide to the final receptor and (2) docking of the pseudopeptide analogues of Ang II in the receptor for comparison with the Ang II binding model.

2.3.1. Docking of the Ang II model peptide to the final receptor structure

An unconstrained conformational analysis of the model peptide Arg-Val-Tyr-Val-His-Pro-Phe was performed in the receptor model, starting in the putative binding pocket previously selected. The ligand and the side chain atoms of Asp^{297}, Asp^{279}, and Lys^{215} were allowed to move. The side chains of the amino acids within 15 Å of the moving atoms were fixed with a force constant of 200 kJ mol^{-1} $Å^{-2}$ but their mutual interactions were kept in the energy calculations (debug switch 17 in BatchMin). The backbone atoms of the receptor residues were frozen during the analysis. The torsion angles and ligand movement were searched with 3400 steps MCMM, altering 2–5 d.o.f. in each step. Energy minimization was performed using TNCG with a maximum of 500 steps and a convergence criterion of 1.0 kJ $Å^{-1}$ mol^{-1}. The OPLS 2005 force field and the GB/SA water solvation model were used in the analysis. The criterion for unique conformations was a minimum atomic separation of 1 Å when comparing the position of $C_{guanidino,Arg}$, $O_{phenol,Tyr}$, $N_{\pi,His}$, $C_{carboxyl,Phe}$, $C4_{Phe}$, $N_{amine,Lys215}$, $C_{carboxyl,Asp279}$, and $C_{carboxyl,Asp297}$. Conformations within 100 kJ/mol of the lowest found energy minimum were saved.

2.3.2. Pseudopeptide docking

Conformational analysis of nine pseudopeptides (**1–9**, Fig. 2) [18–21] was performed in the Ang II binding site of the AT_2 receptor model. The ligand–receptor complex corresponding to ligand conformation 3 in Table 1 was used as a template for building the pseudopeptides. The Asp residue in the pseudopeptides was replaced with an acetyl capping group. The benzodiazepine-based scaffold was built in an inverse γ-turn conformation (equatorial Tyr side chain). Since all ligands have the same three C-terminal residues (His-Pro-Phe), the position of these residues was taken from the docking result of the Ang II model peptide, in order to remove degrees of freedom and focus the analysis on the part of the ligands that differed. Thus, only the atoms of the ligands from the N-terminal up to C_α of His were allowed to move in the analysis, with the surrounding atoms within 15 Å set as frozen. The torsion angles were searched using 200 MCMM search steps per torsion angle, altering 1 to $N - 1$ torsion angles in each step (where N is the number of searched torsion angles). Energy minimization was performed using a maximum of 500 TNCG steps with a 1.0 kJ $Å^{-1}$ mol^{-1} convergence criterion. The OPLS 2005 force field and the GB/SA water solvation model were used in the analysis. The criterion for unique conformations was a minimum atomic separation of 1 Å when comparing the position of $C_{guanidino,Arg}$, $O_{phenol,Tyr}$, $C_{\alpha,His}$, $C_{methyl,acetylcap}$ and $C_{\beta,Val}$ (if present). Conformations within 50 kJ/mol of the lowest found energy minimum were saved.

3. Results

3.1. Building and refinement of the AT_2 receptor model

The initial docking study starting from the extended conformer of the Ang II model peptide when ECL2 was removed resulted in 119 configurations of the ligand–receptor complex. However, since the main objective with this small initial docking was to refine the positioning of ECL2, only the 10 configurations with the lowest energy ($\Delta E = 8$ kcal/mol) were further examined. Geometrical comparison of the extracted ligands showed that they had a backbone conformation similar to the starting conformation (rms atom-pair distance of 1.2–1.7 Å when superimposing the C_α atoms). When ECL2 was mounted on the receptor the only portion of ECL2 in the original conformation not compatible with the ligand conformations was the 188–199 residue segment. This segment was therefore rebuilt with one of the ligand poses included as a boundary. This resulted in four conformational

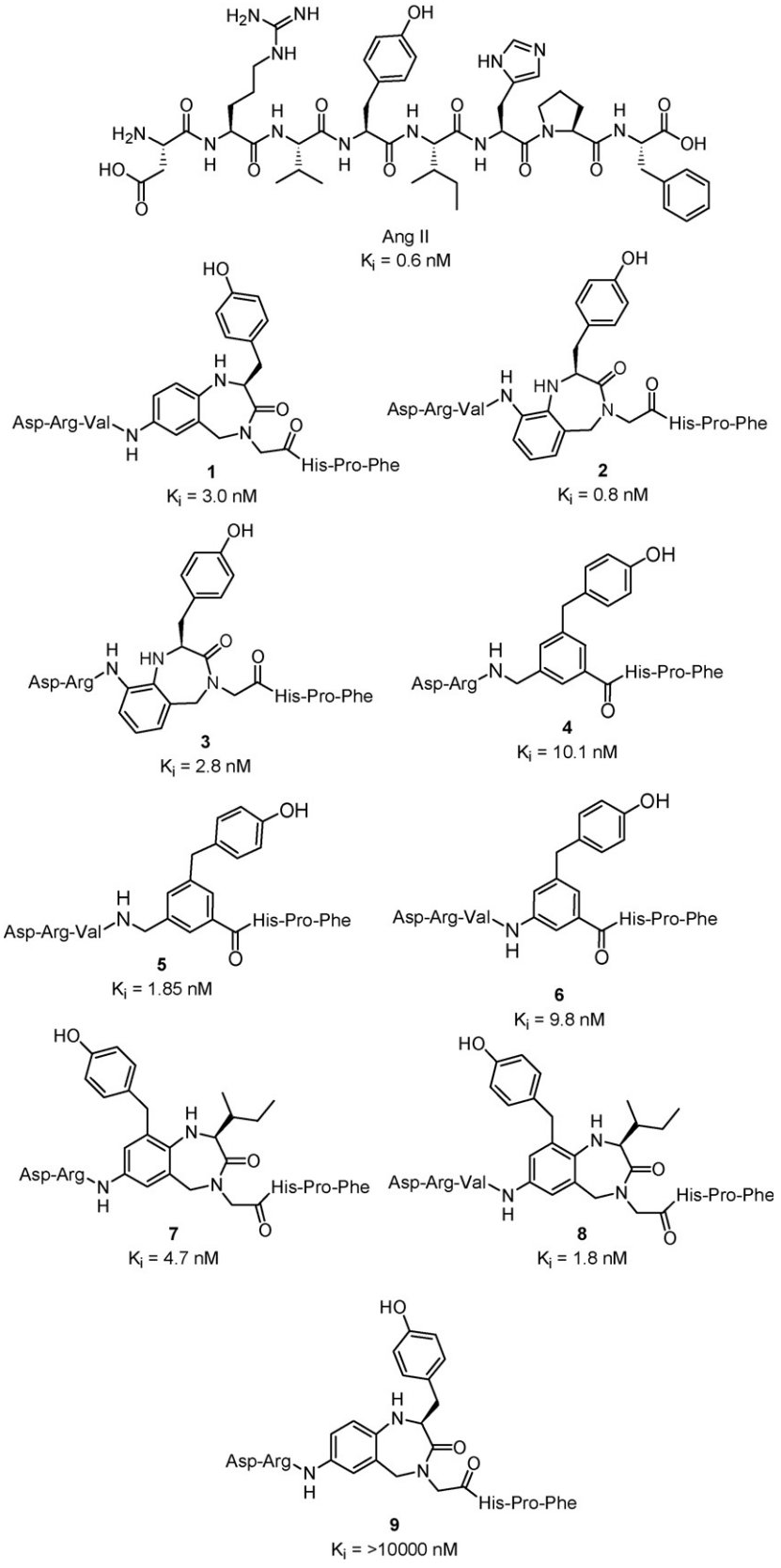

Fig. 2. Angiotensin II and the pseudopeptides used in the modeling along with their AT_2 receptor affinity (pig uterus myometrium).

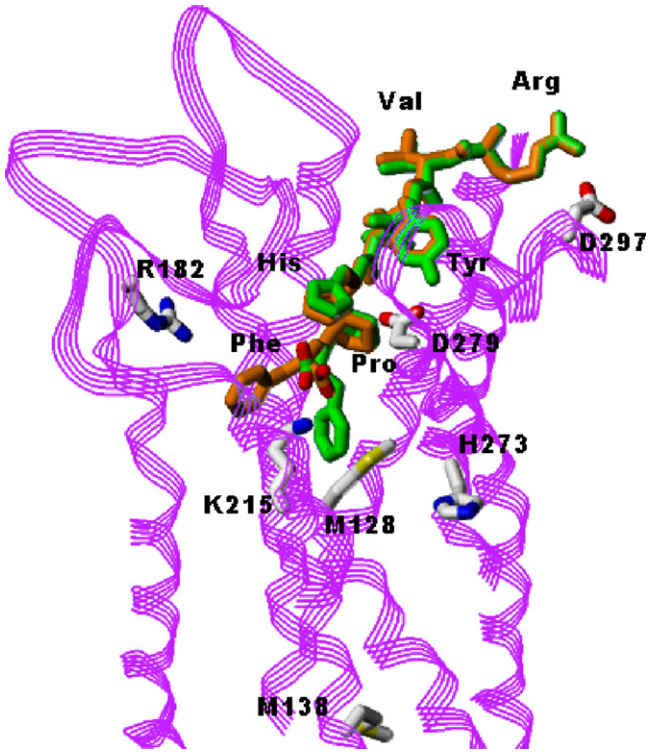

Fig. 3. Sketch of the final AT_2 receptor model shown as purple line ribbons. The ligand conformations corresponding to conformations 2 and 3 in Table 1 are shown in green and orange, respectively, except oxygen atoms of the C-terminal carboxyl group that are shown in red. The contact residues of the receptor suggested by experimental data are shown in conventional atom colors (only side chains shown). All hydrogens are omitted.

clusters of this segment and the most open was selected for the final receptor 3D model (Fig. 3).

3.2. Docking of the Ang II model peptide to the refined AT_2 receptor model

Using the final receptor model, an unconstrained conformational analysis of Arg-Val-Tyr-Val-His-Pro-Phe was performed. In total, 1347 configurations of the ligand–receptor complex were found in the docking. Twenty of the ligand–receptor configurations displayed an unlikely binding mode involving interaction of the Arg side chain with Glu^{45} in the receptor. Glu^{45} is located far from the extracellular cavity of the AT_2 receptor on the outer side of TM1. In all 20 conformations where a Glu^{45} interaction was present, the Arg side chain was positioned on top of TM1, which is not a possible binding mode since in a complete receptor model the N-terminal segment of the AT_2 receptor occupies this space. Thus, these conformations were not considered to be a valid binding mode for the ligand and were removed, leaving 1327 ligand–receptor configurations for further analysis.

As described in Fig. 1, some receptor residues in the TM region and extracellular loops, namely Met^{128} and Met^{138} [31], Arg^{182} [24,25], Lys^{215} [26,27], His^{273} [28], Asp^{279} [30], and Asp^{297} [25,29], were suggested to participate in Ang II–AT_2 receptor interactions. The 1327 ligand–receptor configurations were analyzed by measuring the distance between the suggested ligand–receptor contact points. These distances were Phe-Met^{128} (represented by atom-pair *para*-H_{Phe}–S_{Met128}), Phe-Met^{138} (*para*-H_{Phe}–S_{Met138}), Tyr-Arg^{182} ($O_{phenol,Tyr}$–$C_{guanidino,Arg182}$), Phe-Lys^{215} ($C_{carboxyl,Phe}$–$N_{amine,Lys215}$), Phe-His^{273} ($C_{\beta,Phe}$–$C_{\beta,His273}$), His-Asp^{279} ($N_{\pi,His}$–$C_{carboxyl,Asp279}$), and Arg-Asp^{297} ($C_{guanidino,Arg}$–$C_{carboxyl,Asp297}$). In addition, during visual inspection of the results several other ligand contacts or proximities with the important receptor residues were found with high occurrence, and were thus included in the analysis. These were Arg-Asp^{279} (atom-pairs $C_{guanidino,Arg}$–$C_{carboxyl,Asp279}$), Tyr-Asp^{297} ($O_{phenol,Tyr}$–$C_{carboxyl,Asp297}$), Tyr-Asp^{279} ($O_{phenol,Tyr}$–$C_{carboxyl,Asp279}$), and Phe-Arg^{182} ($C_{\alpha,Phe}$–$C_{guanidino,Arg182}$).

Visual inspection of the clusters of short atom-pair distances was performed, which suggested that a specific distance range could be used to define some of the ligand–receptor contacts. These distance ranges were defined as less than 5 Å for a $C_{guanidino}$–$C_{carboxyl}$ distance and less than 4 Å for a $C_{carboxyl}$-heteroatom distance (i.e., measured distances including His, Lys and Tyr residues). Furthermore, guided by the reaction radius in the photoaffinity labeling study, the definition for a Phe-Met contact was set to a distance of maximum 6 Å.

The docking results showed that several of the proposed contact points of Ang II with the AT_2 receptor were accounted for in the ligand–receptor complexes. Using the defined distances of ligand–receptor contacts, the Phe(carboxyl)-Lys^{215} ionic bridge was the most frequently occurring in the ligand–receptor configurations (1277 of 1327), followed by the His-Asp^{279} (745) and Arg-Asp^{297} (627) contacts. For the Tyr residue, contacts with Asp^{279} were the most frequent among the investigated contacts (129). In some of the ligand–receptor complexes, interactions between Tyr-Asp^{297} (76) and Arg-Asp^{279} (36) could also be found. In total, 494 ligand–receptor configurations had three or more contacts between the ligand and important residues in the AT_2 receptor, 549 had two, 273 had one, and 11 had zero contacts. Only one configuration had a Phe-Met^{128} contact. Interestingly, this configuration also had ligand contact with Asp^{279}, Lys^{215}, and Asp^{297}. In addition, this configuration had the closest distance between Phe and His^{273} (9.8 Å $C_{\beta,Phe}$–$C_{\beta,His273}$) and the ligand was also in proximity of Arg^{182}. The dihedral angles of the backbone defining the ligand conformation are listed in Table 1 as conformation 2. Disappointingly, this configuration had a high relative energy (ΔE = 23 kcal/mol). However, a very similar ligand–receptor configuration with a low energy (ΔE = 0.8 kcal/mol) was also identified and the ligand conformation is listed in Table 1 as conformation 3. The only difference between the two conformations was the relative geometry of the Phe residue (Fig. 3). The AT_2 receptor residues in the region around Phe are closely packed with the ligand and this may greatly affect the energy of the complex if the receptor is allowed to move. Thus we believe that both of these configurations are probable binding modes for Ang II. Compared to the initially derived Ang II binding model (conformation 1, Table 1) the backbone dihedral angles differ from these two ligand conformations

but the overall backbone orientation is similar, with an rms atom-pair distance of 1.7–1.8 Å when superimposing the C_α atoms.

In summary, these two conformations can interact with Met^{128}, Lys^{215}, Asp^{279}, and Asp^{297} and show proximity to Arg^{182} and His^{273}. Also notably, an inverse γ-turn conformation is formed around the Tyr residue in these conformations, in accordance with previous modeling studies of cyclized Ang II analogues [51] and the pseudopeptides comprising a γ-turn mimetic moiety in this study. Both structures of the ligand–receptor complex configurations can be requested from the corresponding author.

3.3. Pseudopeptide binding

To investigate whether the pseudopeptides (**1**–**8**) could adopt the same binding mode as Ang II they were docked to the AT_2 receptor model. To facilitate the docking analysis, the His-Pro-Phe fragment was constrained to the position of the His-Pro-Phe fragment obtained from the docked Ang II model peptide (conformation 3, Table 1). The inactive pseudopeptide **9** was also included in the analysis in an attempt to rationalize the inactivity of this compound. For each of the pseudopeptides **1**–**9**, 129, 168, 163, 114, 226, 96, 126, 90, and 14 conformations, respectively, were identified within 10 kcal/mol of the lowest energy configuration. These conformations were analyzed by extracting and exporting the conformations to SYBYL [52] and performing a comparison with the binding mode attained by the Ang II model peptide (conformation 3 in Table 1). In the comparison we focused on the positions of the Arg and Tyr side chains by measuring the $O_{phenol,Tyr}$–$O_{phenol,Tyr}$ and $C_{guanidine,Arg}$–$C_{guanidine,Arg}$ atom-pair distances between the conformations of each pseudopeptide and the Ang II binding model. The comparison showed that all pseudopeptides had conformations that could position the Arg guanidino group within 1.5 Å of the position of this group in the Ang II binding model. When considering the positioning of both the Arg and Tyr side chains, conformations of **1** and **3** were found to fully match the Ang II model, obtaining a direct contact with Asp^{279} and Asp^{297}. Pseudopeptides **2** and **5** were partly matched to this model, with their Tyr residues in the same area of the receptor but not with the same Tyr-Asp^{279} interaction as the Ang II model. The Val residue present in **1**, **2** and **5** were found in proximity to Ile^{47}, which may be an additional ligand–receptor interaction for these compounds. The ligand–receptor configurations of the Ang II model peptide, **1**, **2**, **3** and **5** are presented in Fig. 4. These models fulfill most of the contact points previously discussed, especially when considering the alternative positioning of the Phe side chain seen in Fig. 3.

None of the conformations of **4**, **6**, **7** and **8** could be matched to the Ang II model when considering the positioning of both the Arg and Tyr side chains. The analysis of these structures was instead focused on conformations that could obtain the Arg-Asp^{297} interaction. This analysis resulted in 7, 6, 38 and 35 conformations of **4**, **6**, **7** and **8**, respectively, that positioned the Arg guanidino group within 5 Å of the corresponding position in the Ang II binding model. When the conformations of these

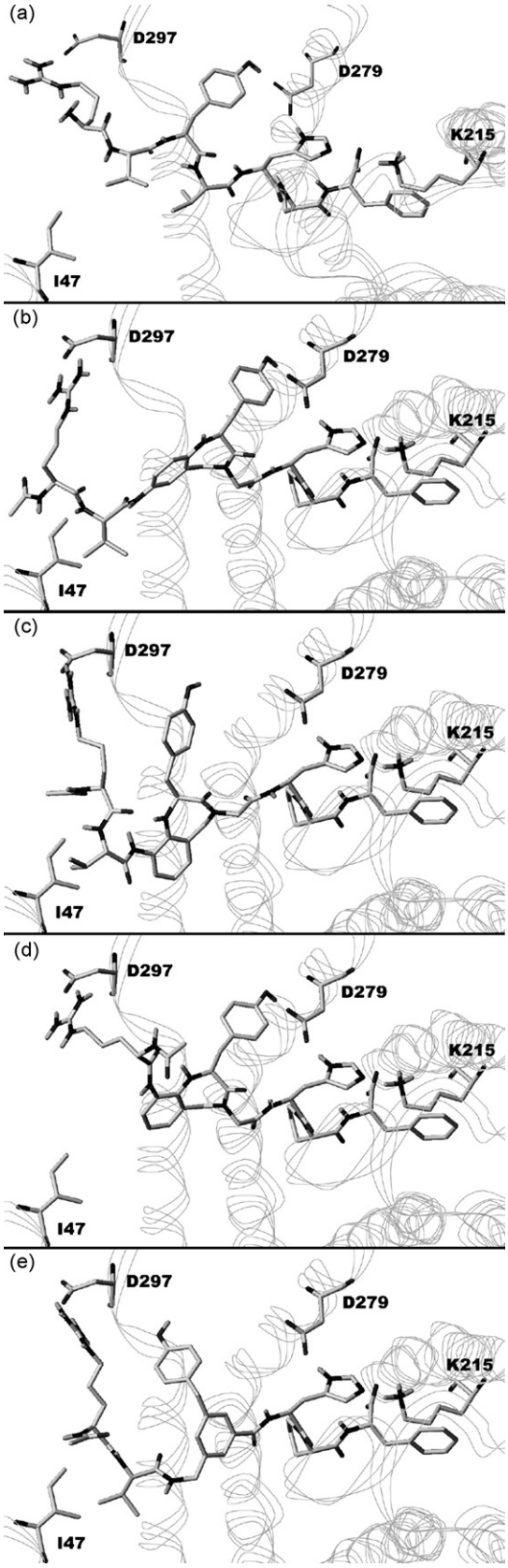

Fig. 4. Ligand configurations for the Ang II model peptide (a) and pseudopeptides **1** (b), **2** (c), **3** (d), and **5** (e). The receptor residues Ile^{47}, Lys^{215}, Asp^{279}, and Asp^{297} are also shown. Only essential hydrogen atoms are shown.

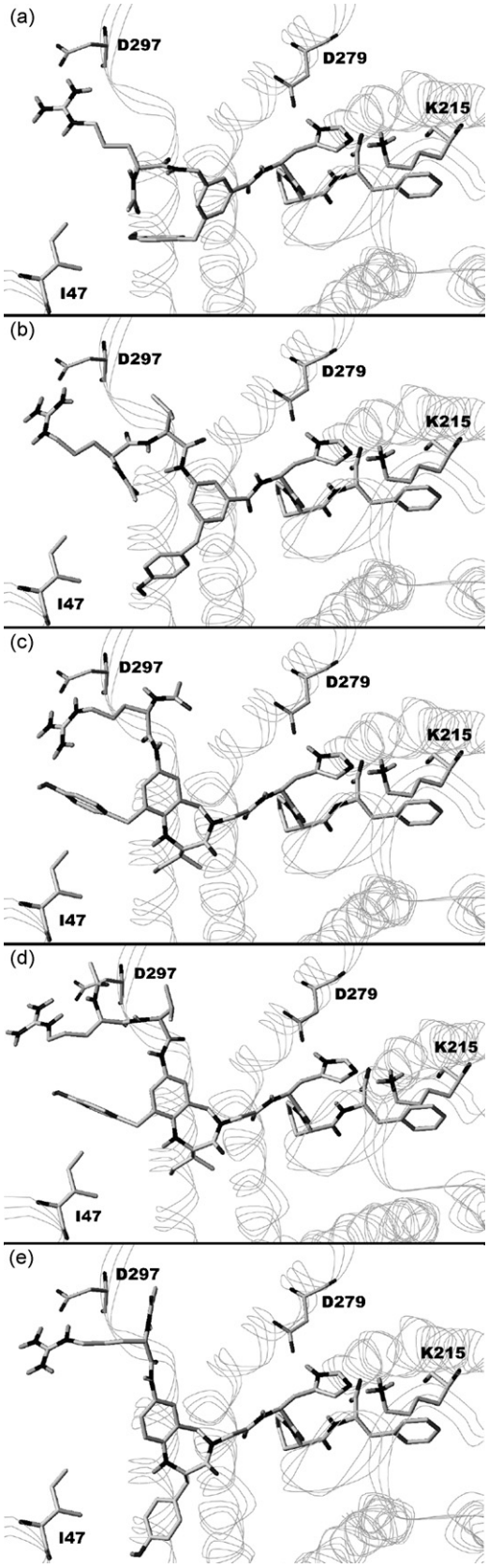

Fig. 5. Ligand configurations showing an alternative binding mode for pseudopeptides **4** (a), **6** (b), **7** (c), **8** (d), and **9** (e). The receptor residues Ile^{47}, Lys^{215}, Asp^{279}, and Asp^{297} are also shown. Only essential hydrogen atoms are shown.

pseudopeptides were examined it was apparent that to be able to obtain the Arg-Asp^{297} interaction the scaffold was rotated, positioning the Tyr side chain far from the position in the Ang II model. The inactive compound **9** also adopted a similar binding configuration, making it difficult to rationalize the inactivity of this compound based on this binding mode. The ligand–receptor configurations of **4**, **6**, **7**, **8**, and **9** are presented in Fig. 5.

4. Discussion

4.1. Flexibility in the extracellular region of the AT_2 receptor

The region of the AT_2 receptor responsible for the initial binding of ligands such as Ang II consists of the extracellular loops and the N-terminal segment. While the conformational flexibility of each loop is somewhat constrained by connections with two TM helices immobilized in the membrane, the N-terminal segment may have much more flexibility. One can assume that whatever binding mode Ang II adopts in the AT_2 receptor, the N-terminal segment will always be able to adjust to this mode due to the high conformational flexibility in this region. This was the main reason why we did not include the N-terminal segment of the receptor in the building process. It has been suggested that in addition to the conserved Cys^{117}-Cys^{195} disulfide bridge in the AT_2 receptor, a second disulfide bridge between Cys^{35} in the N-terminal segment of the AT_2 receptor can form a disulfide bridge with Cys^{290} in ECL3. Even if this additional disulfide bridge would reduce the flexibility of these segments, the importance of this disulfide bridge is unclear as shown by a higher Ang II affinity to AT_2 receptor mutants where Cys^{35} and Cys^{290} are replaced by Ala [53,54]. Also, it has been shown that AT_2 receptors can homo-oligomerize, forming an intermolecular disulfide bridge between the Cys^{35} residue in one AT_2 receptor and the Cys^{290} residue in other AT_2 receptor [55]. Thus the roll and occurrence of the intramolecular Cys^{35}-Cys^{290} disulfide bridge seem unclear.

The loops are presumably not as flexible as the N-terminal segment, but, on the other hand, the snapshots of the extracellular loops presented in the X-ray structure of rhodopsin are likely not representative of the situation in a complex with a rather large octapeptide ligand such as Ang II. It seems much more likely that the loops need to be in an ‘‘open’’ conformation at some stage during the initial binding of Ang II. Thus, rather than using the conformations of the loops in the crystallized rhodopsin structure, the loops were modeled using a build-up procedure. Energy calculations performed for the ECL1 + ECL2 + ECL3 package, in the absence of Ang II, showed that in all low-energy structures the ECLs are tightly packed, and therefore do not provide a suitable binding pocket for Ang II. Therefore, modeling studies of the interaction of Ang II with the AT_2 receptor started from docking a model peptide of Ang II with the most ‘‘open’’ conformation of ECL1 + ECL2 + ECL3 found. The final receptor structure was derived by including the docked ligand when building the ECLs. This made the receptor model suitable for ligand

docking, at least for modeling the initial binding mode of the ligands. An earlier modeling approach to the AT_2 receptor [16] used the positioning of the loops as they were presented in the X-ray template of rhodopsin, so that the ligand had to be placed in the ''closed'' receptor before applying energy minimization. Thus, our approach may more closely mimic the ligand binding event. It should be noted that results of our modeling correspond to the resting state of the AT_2 receptor, since the receptor model was built based on the template of the dark-adapted rhodopsin. The activation process of GPCRs is proposed to involve several intermediate receptor conformations, induced or stabilized by an agonist that disrupts the intramolecular bond network in the receptor [56]. Our partial AT_2 receptor model is thus more suitable to describe the initial ligand binding rather than the conformational transitions in the AT_2 receptor during activation and therefore, this model may not be suitable for determining the binding mode of the ligands when the receptor is activated (the ''off'' stage of the on/off process).

4.2. Ang II binding

The conformational analysis of the model peptide of Ang II in the final receptor model resulted in a number of interesting binding models. In general, the positioning of the suggested ligand–receptor contact points Arg-Asp^{297} and Phe-Lys^{215} was only compatible with an extended conformation of the ligand. In all low-energy models, Phe was positioned close to Lys^{215} with an ionic bridge between the C-terminal carboxyl group of Ang II and the amino group of the Lys^{215} residue. For the Phe side chain, two reasonable binding modes were found, one on each side of the Lys^{215} side chain. One binding mode was present in all low-energy models, where the side chain was positioned in a relatively small pocket. In one of the models with higher energy, the Phe side chain was instead positioned towards a larger pocket, pointing downwards in the TM region. In this binding mode the Phe side chain is in contact with Met^{128} and much closer to the His^{273} residue, which are two suggested contact points for Ang II. Thus, this binding mode of Phe looks reasonable. However, depending on the receptor movement in general or during activation, Ang II and/or different analogues may be able to bind in both ways with a good fit to the receptor. Therefore, we consider the two models depicted in Fig. 3 as the most plausible 3D models for the complex of Ang II with the AT_2 receptor derived in this study, since these models include contacts of Ang II with almost all receptor residues suggested as contact points by experimental data (Met^{128}, Lys^{215}, Asp^{279}, and Asp^{297} and proximity to Arg^{182} and His^{273}). Although the docking results are supported by most of the available experimental data, more experimental data are desired in order to increase the reliability of the derived models, especially data that indicate specific ligand–receptor contacts.

It should be noted that even though most of the experimental data supports the current models, some of the reported results cannot be explained by this model. Ligand contact with Met^{138} seems especially difficult to obtain with our model. Met^{138} is far down in the TM region and would require massive movement of the TM side chains to position the Phe side chain in the vicinity of this residue. Furthermore, Arg^{182} is not in direct contact with the ligand in any configuration found. This residue is somewhat shielded by ECL2, which is not freely movable because of the disulfide bridge between this loop and TM3. From studies of Ang II interactions with the AT_1 receptor [57], Arg^{182} is speculated to interact with Tyr in Ang II when binding to the AT_2 receptor [24,25]. This seems unlikely from the results in the present study. Instead our calculations indicate that the Phe residue of Ang II is closer to Arg^{182}, which may be a possible contact if any direct ligand–receptor interaction exists with Arg^{182}.

4.3. Pseudopeptide binding

When comparing the pseudopeptides with the Ang II binding model, all compounds are able to obtain a common Arg-Asp^{297} interaction. In general, the ligands comprising the benzodiazepine-based γ-turn mimetic seem to most closely mimic the presented binding mode of Ang II. For some of the ligands (**4**, **6**, **7**, and **8**), the Tyr residues are, however, oriented very differently compared to the Ang II binding model. The inactive compound **9** also adopts a similar conformation as **4**, **6**, **7**, and **8** in the conformations where an Arg-Asp^{297} interaction is present, which makes it difficult to rationalize the inactivity of this compound based on this binding mode. However, **9** is the compound that has the Tyr side chain deepest in the TM region, which may result in non-optimal interactions with the receptor. It also adopts the energetically less favorable classic γ-turn conformation with an axial Tyr side chain, which can contribute to the inactivity of this compound. The docking poses of compounds **7** and **8**, comprising the β-turn mimic scaffold, also adopt the energetically less favorable conformation with an axial side chain in the scaffold, but with Ile instead of Tyr in this position. Thus one possible reason for the difference in affinity of **7** and **8** compared to **9** is less steric clash with the receptor. We recently published a ligand-based model using **1**–**6** and superimposed **7** and **8** to this model. It was suggested that all pseudopeptides **1**–**8** could obtain a similar binding mode in the AT_2 receptor, including the alignment of both the Arg and Tyr residues [18,19]. Even though the pseudopeptides have high AT_2 receptor affinity and contain similar side chains, their geometry in the turn mimetic region around Tyr are noticeably different, both regarding the positioning of the Tyr side chain and the direction and length of the peptide backbone. In the present study when the His-Pro-Phe residues in the pseudopeptides were forced to adopt the same position as the docked Ang II model peptide no common alignment of the Tyr residue could be identified. However, in a dynamic binding process such an exact positioning of the C-terminal fragments will likely not occur and these amino acids may reposition so that a common alignment of Tyr can be obtained. On the other hand, amino acid scans of Ang II have shown that no single amino acid is of vast importance for high AT_2 receptor affinity. Thus, the different positions observed for the Tyr side chain may not be of great importance as long as other contacts can still be achieved, e.g., with Arg, His, Pro and Phe.

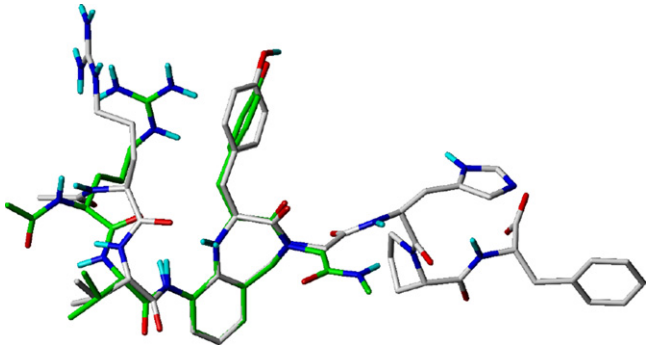

Fig. 6. Comparison between a previously derived ligand-based binding model (green carbons) and the structure-based model (white carbons) obtained herein. Compound **2** is shown.

Four of the pseudopeptides (**1**, **2**, **3**, and **5**) could all adopt similar binding modes as found for the Ang II model peptide. A comparison of the binding mode obtained from docking in the AT_2 receptor and from the model derived using the ligand-based approach is shown in Fig. 6, where the benzodiazepine-based scaffold of **2** from each model is superimposed. From this comparison it can be seen that the models are very similar. The main difference lies in the backbone torsion angle in the outgoing C-terminal part of the benzodiazepine scaffold. Importantly, we are now able to incorporate a hypothesis concerning the outgoing direction and conformation of the C-terminal His-Pro-Phe fragment to the indirect model.

The valine residue present in **1** was previously thought to introduce some flexibility in the backbone between Arg and Tyr to enable a favorable ligand–receptor interaction, such as the Arg-Asp^{297} interaction [20]. This hypothesis is now supported in the docked conformations of **1**. Also, the valine side chain in **1**, **2** and **5** are oriented towards Ile^{47} (Fig. 4) in the receptor, which could explain some of the increased affinity when a valine residue is present in the pseudopeptides, which has also been suggested before [21].

5. Conclusions

In summary, we have explored binding modes of Ang II and pseudopeptide Ang II analogues in the AT_2 receptor model, taking into account also the conformational flexibility of the extracellular loops. The AT_2 receptor was built using the bovine rhodopsin receptor structure as a template for the transmembrane helical domain. The extracellular loops were added using a build-up procedure to create a receptor structure suitable for docking studies. From the docking of an Ang II model peptide, several ligand–receptor contacts were found that were in agreement with experimental data. Furthermore, nine pseudopeptide Ang II analogues were docked in the receptor but only four of these adopted a similar binding mode as compared to Ang II. Interestingly, this binding mode was similar to the binding model of these analogues that was derived without knowledge of the 3D structure of the AT_2 receptor.

Acknowledgments

We gratefully acknowledge support from the Swedish Foundation for Strategic Research. The authors also thank Shane Peterson and Dr. Martin Almlöf for proof-reading of the paper.

Appendix A. Supplementary data

Supplementary data associated with this article can be found, in the online version, at doi:10.1016/j.jmgm.2007.08.005.

References

[1] E. Kaschina, T. Unger, Angiotensin AT_1/AT_2 receptors: regulation, signalling and function, Blood Press. 12 (2003) 70–88.
[2] M. De Gasparo, K.J. Catt, T. Inagami, J.W. Wright, T. Unger, International union of pharmacology. XXIII. The angiotensin II receptors, Pharmacol. Rev. 52 (2000) 415–472.
[3] M. Mukoyama, M. Nakajima, M. Horiuchi, H. Sasamura, R.E. Pratt, V.J. Dzau, Expression cloning of type 2 angiotensin II receptor reveals a unique class of seven-transmembrane receptors, J. Biol. Chem. 268 (1993) 24539–24542.
[4] Y. Kambayashi, S. Bardhan, K. Takahashi, S. Tsuzuki, H. Inui, T. Hamakubo, T. Inagami, Molecular cloning of a novel angiotensin II receptor isoform involved in phosphotyrosine phosphatase inhibition, J. Biol. Chem. 268 (1993) 24543–24546.
[5] K.L. Spear, M.S. Brown, E.J. Reinhard, E.G. McMahon, G.M. Olins, M.A. Palomo, D.R. Patton, Conformational restriction of angiotensin II: cyclic analogues having high potency, J. Med. Chem. 33 (1990) 1935–1940.
[6] P. Johannesson, G. Lindeberg, A. Johansson, G.V. Nikiforovich, A. Gogoll, B. Synnergren, M. Le Greves, F. Nyberg, A. Karlén, A. Hallberg, Vinyl sulfide cyclized analogues of angiotensin II with high affinity and full agonist activity at the AT_1 receptor, J. Med. Chem. 45 (2002) 1767–1777.
[7] K. Plucinska, T. Kataoka, M. Yodo, W.L. Cody, J.X. He, C. Humblet, G.H. Lu, E. Lunney, T.C. Major, R.L. Panek, P. Schelkum, R. Skeean, G.R. Marshall, Multiple binding modes for the receptor-bound conformations of cyclic AII agonists, J. Med. Chem. 36 (1993) 1902–1913.
[8] E.E. Sugg, C.A. Dolan, A.A. Patchett, R.S.L. Chang, K.A. Faust, V.J. Lotti, In peptides, chemistry, structure biology, pp. 305–306, in: J.E. Rivier, G.R. Marshall (Eds.), Proceedings of the 11th American Peptide Symposium, ESCOM, Leiden, 1990.
[9] J.M. Samanen, C.E. Peishoff, R.M. Keenan, J. Weinstock, Refinement of a molecular model of angiotensin II (AII) employed in the discovery of potent nonpeptide antagonists, Bioorg. Med. Chem. Lett. 3 (1993) 909–914.
[10] G.V. Nikiforovich, J.L.F. Kao, K. Plucinska, W.J. Zhang, G.R. Marshall, Conformational analysis of two cyclic analogs of angiotensin: implications for the biologically active conformation, Biochemistry 33 (1994) 3591–3598.
[11] B. Schmidt, S. Lindman, W. Tong, G. Lindeberg, A. Gogoll, Z. Lai, M. Thornwall, B. Synnergren, A. Nilsson, C.J. Welch, M. Sohtell, C. Westerlund, F. Nyberg, A. Karlén, A. Hallberg, Design, synthesis, and biological activities of four angiotensin II receptor ligands with γ-turn mimetics replacing amino acid residues 3–5, J. Med. Chem. 40 (1997) 903–919.
[12] M.P. Printz, G. Némethy, H. Bleich, Proposed models for angiotensin II in aqueous solution and conclusions about receptor topography, Nat. New Biol. 237 (1972) 135–140.
[13] S. Lindman, G. Lindeberg, F. Nyberg, A. Karlén, A. Hallberg, Comparison of three γ-turn mimetic scaffolds incorporated into angiotensin II, Bioorg. Med. Chem. 8 (2000) 2375–2383.
[14] G.V. Nikiforovich, G.R. Marshall, Three-dimensional recognition requirements for angiotensin agonists: a novel solution for an old problem, Biochem. Biophys. Res. Commun. 195 (1993) 222–228.

[15] M. Clement, S.S. Martin, M.-E. Beaulieu, C. Chamberland, P. Lavigne, R. Leduc, G. Guillemette, E. Escher, Determining the environment of the ligand binding pocket of the human angiotensin II type I (hAT_1) receptor using the methionine proximity assay, J. Biol. Chem. 280 (2005) 27121–27129.
[16] M. Deraet, L. Rihakova, A. Boucard, J. Perodin, S. Sauve, A.P. Mathieu, G. Guillemette, R. Leduc, P. Lavigne, E. Escher, Angiotensin II is bound to both receptors AT_1 and AT_2, parallel to the transmembrane domains and in an extended form, Can. J. Physiol. Pharmacol. 80 (2002) 418–425.
[17] P. Johannesson, G. Lindeberg, M. Erdélyi, P.-A. Frändeberg, A. Karlén, A. Hallberg, AT_2 selective angiotensin II analogues encompassing tyrosine functionalized 5,5-bicyclic thiazabicycloalkane dipeptide mimetics, J. Med. Chem. 47 (2004) 6009–6019.
[18] J. Georgsson, C. Sköld, B. Plouffe, G. Lindeberg, M. Botros, M. Larhed, F. Nyberg, N. Gallo-Payet, A. Karlén, A. Hallberg, Angiotensin II pseudopeptides containing 1,3,5 trisubstituted benzene scaffolds with high AT_2 receptor affinity, J. Med. Chem. 48 (2005) 6620–6631.
[19] U. Rosenstrom, C. Skold, G. Lindeberg, M. Botros, F. Nyberg, A. Karlen, A. Hallberg, Design, synthesis, and incorporation of a beta-turn mimetic in angiotensin II forming novel pseudopeptides with affinity for AT_1 and AT_2 receptors, J. Med. Chem. 49 (2006) 6133–6137.
[20] U. Rosenström, C. Sköld, G. Lindeberg, M. Botros, F. Nyberg, A. Karlén, A. Hallberg, A selective AT_2 receptor ligand with a γ-turn-like mimetic replacing the amino acid residues 4–5 of angiotensin II, J. Med. Chem. 47 (2004) 859–870.
[21] U. Rosenström, C. Sköld, B. Plouffe, H. Beaudry, G. Lindeberg, M. Botros, F. Nyberg, G. Wolf, A. Karlén, N. Gallo-Payet, A. Hallberg, New selective AT_2 receptor ligands encompassing a γ-turn mimetic replacing the amino acid residues 4–5 of angiotensin II act as agonists, J. Med. Chem. 48 (2005) 4009–4024.
[22] U. Rosenström, C. Sköld, G. Lindeberg, M. Botros, F. Nyberg, A. Hallberg, A. Karlén, Synthesis and AT_2 receptor binding properties of angiotensin II analogues, J. Pept. Res. 64 (2004) 194–201.
[23] S.-I. Miura, S.S. Karnik, Angiotensin II type 1 and type 2 receptors bind angiotensin II through different types of epitope recognition, J. Hypertens. 17 (1999) 397–404.
[24] J. Kurfis, D. Knowle, L. Pulakat, Role of Arg182 in the second extracellular loop of angiotensin II receptor AT_2 in ligand binding, Biochem. Biophys. Res. Commun. 263 (1999) 816–819.
[25] J.N. Heerding, D.K. Yee, S.L. Jacobs, S.J. Fluharty, Mutational analysis of the angiotensin II type 2 receptor: contribution of conserved extracellular amino acids, Regul. Pept. 72 (1997) 97–103.
[26] L. Pulakat, A.S. Tadessee, J.J. Dittus, N. Gavini, Role of Lys^{215} located in the fifth transmembrane domain of the AT_2 receptor in ligand-receptor interaction, Regul. Pept. 73 (1998) 51–58.
[27] D.K. Yee, L.R. Kisley, J.N. Heerding, S.J. Fluharty, Mutation of a conserved fifth transmembrane domain lysine residue (Lys^{215}) attenuates ligand binding in the angiotensin II type 2 receptor, Mol. Brain Res. 51 (1997) 238–241.
[28] C.A. Turner, S. Cooper, L. Pulakat, Role of the His273 located in the sixth transmembrane domain of the angiotensin II receptor subtype AT_2 in ligand-receptor interaction, Biochem. Biophys. Res. Commun. 257 (1999) 704–707.
[29] D. Knowle, J. Kurfis, N. Gavini, L. Pulakat, Role of Asp297 of the AT_2 receptor in high-affinity binding to different peptide ligands, Peptides 22 (2001) 2145–2149.
[30] J.N. Heerding, D.K. Yee, M.Z. Krichavsky, S.J. Fluharty, Mutational analysis of the angiotensin type 2 receptor: contribution of conserved amino acids in the region of the sixth transmembrane domain, Regul. Pept. 74 (1998) 113–119.
[31] L. Rihakova, M. Deraet, M. Auger-Messier, J. Perodin, A. Boucard Antony, G. Guillemette, R. Leduc, P. Lavigne, E. Escher, Methionine proximity assay, a novel method for exploring peptide ligand-receptor interaction, J. Recept. Signal Transduct. Res. 22 (2002) 297–313.
[32] G. Servant, S.A. Laporte, R. Leduc, E. Escher, G. Guillemette, Identification of angiotensin II-binding domains in the rat AT_2 receptor with photolabile angiotensin analogs, J. Biol. Chem. 272 (1997) 8653–8659.
[33] U. Gether, Uncovering molecular mechanisms involved in activation of G protein-coupled receptors, Endocr. Rev. 21 (2000) 90–113.
[34] K. Palczewski, T. Kumasaka, T. Hori, C.A. Behnke, H. Motoshima, B.A. Fox, I. Le Trong, D.C. Teller, T. Okada, R.E. Stenkamp, M. Yamamoto, M. Miyano, Crystal structure of rhodopsin: a G protein-coupled receptor, Science 289 (2000) 739–745.
[35] C. Baleanu-Gogonea, S. Karnik, Model of the whole rat AT_1 receptor and the ligand-binding site, J. Mol. Model. 12 (2006) 325–337.
[36] G.V. Nikiforovich, G.R. Marshall, 3D model for TM region of the AT-1 receptor in complex with angiotensin II independently validated by site-directed mutagenesis data, Biochem. Biophys. Res. Commun. 286 (2001) 1204–1211.
[37] G.V. Nikiforovich, G.R. Marshall, Three-dimensional model for meta-II rhodopsin, an activated G-protein-coupled receptor, Biochemistry 42 (2003) 9110–9120.
[38] G.V. Nikiforovich, G.R. Marshall, Modeling flexible loops in the dark-adapted and activated states of rhodopsin, a prototypical G-protein-coupled receptor, Biophys. J. 89 (2005) 3780–3789.
[39] L.G. Dunfield, A.W. Burgess, H.A. Scheraga, Energy parameters in polypeptides. 8. Empirical potential energy algorithm for the conformational analysis of large molecules, J. Phys. Chem. 82 (1978) 2609–2616.
[40] G. Nemethy, M.S. Pottle, H.A. Scheraga, Energy parameters in polypeptides. 9. Updating of geometrical parameters, nonbonded interactions, and hydrogen bond interactions for the naturally occurring amino acids, J. Phys. Chem. 87 (1983) 1883–1887.
[41] http://ca.expasy.org/tools.
[42] G.V. Nikiforovich, V.J. Hruby, O. Prakash, C.A. Gehrig, Topographical requirements for d-selective opioid peptides, Biopolymers 31 (1991) 941–955.
[43] G.V. Nikiforovich, Computational molecular modeling in peptide drug design, Int. J. Pept. Protein Res. 44 (1994) 513–531.
[44] S. Lindman, G. Lindeberg, P.-A. Frandberg, F. Nyberg, A. Karlen, A. Hallberg, Effect of 3–5 monocyclizations of angiotensin II and 4-AminoPhe6-Ang II on AT_2 receptor affinity, Bioorg. Med. Chem. 11 (2003) 2947–2954.
[45] MacroModel, version 9.1, Schrödinger, LLC, New York, NY, 2005.
[46] G.A. Kaminski, R.A. Friesner, J. Tirado-Rives, W.L. Jorgensen, Evaluation and reparametrization of the OPLS-AA force field for proteins via comparison with accurate quantum chemical calculations on peptides, J. Phys. Chem. B 105 (2001) 6474–6487.
[47] J.W. Ponder, F.M. Richards, An efficient Newton-like method for molecular mechanics energy minimization of large molecules, J. Comput. Chem. 8 (1987) 1016–1024.
[48] M. Saunders, K.N. Houk, Y.D. Wu, W.C. Still, M. Lipton, G. Chang, W.C. Guida, Conformations of cycloheptadecane: a comparison of methods for conformational searching, J. Am. Chem. Soc. 112 (1990) 1419–1427.
[49] G. Chang, W.C. Guida, W.C. Still, An internal-coordinate Monte Carlo method for searching conformational space, J. Am. Chem. Soc. 111 (1989) 4379–4386.
[50] W.C. Still, A. Tempczyk, R.C. Hawley, T. Hendrickson, Semianalytical treatment of solvation for molecular mechanics and dynamics, J. Am. Chem. Soc. 112 (1990) 6127–6129.
[51] S. Lindman, G. Lindeberg, A. Gogoll, F. Nyberg, A. Karlen, A. Hallberg, Synthesis, receptor binding affinities and conformational properties of cyclic methylenedithioether analogs of angiotensin II, Bioorg. Med. Chem. 9 (2001) 763–772.
[52] SYBYL 7.1, Tripos Inc., St. Louis, MO, USA.
[53] J.N. Heerding, J. Hines, S.J. Fluharty, D.K. Yee, Identification and function of disulfide bridges in extracellular domains of angiotensin II type 2 receptor, Biochemistry 40 (2001) 8369–8377.
[54] Y.H. Feng, Y. Saad, S.S. Karnik, Reversible inactivation of AT_2 angiotensin II receptor from cysteine-disulfide bond exchange, FEBS Lett. 484 (2000) 133–138.
[55] S.-i. Miura, S.S. Karnik, K. Saku, Constitutively active homo-oligomeric angiotensin II type 2 receptor induces cell signaling independent of

receptor conformation and ligand stimulation, J. Biol. Chem. 280 (2005) 18237–18244.

[56] B.K. Kobilka, X. Deupi, Conformational complexity of G-protein-coupled receptors, Trends Pharmacol. Sci. 28 (2007) 397–406.

[57] Y. Yamano, K. Ohyama, M. Kikyo, T. Sano, Y. Nakagomi, Y. Inoue, N. Nakamura, I. Morishima, D.F. Guo, T. Hamakubo, Mutagenesis and the molecular modeling of the rat angiotensin II receptor (AT_1), J. Biol. Chem. 270 (1995) 14024–14030.